

University of Groningen

Surface-confined molecular assembly

Enache, Mihaela

IMPORTANT NOTE: You are advised to consult the publisher's version (publisher's PDF) if you wish to cite from it. Please check the document version below.

Document Version

Publisher's PDF, also known as Version of record

Publication date:

2016

[Link to publication in University of Groningen/UMCG research database](#)

Citation for published version (APA):

Enache, M. (2016). *Surface-confined molecular assembly: Investigations with local and non-local probes*. University of Groningen.

Copyright

Other than for strictly personal use, it is not permitted to download or to forward/distribute the text or part of it without the consent of the author(s) and/or copyright holder(s), unless the work is under an open content license (like Creative Commons).

The publication may also be distributed here under the terms of Article 25fa of the Dutch Copyright Act, indicated by the "Taverne" license. More information can be found on the University of Groningen website: <https://www.rug.nl/library/open-access/self-archiving-pure/taverne-amendment>.

Take-down policy

If you believe that this document breaches copyright please contact us providing details, and we will remove access to the work immediately and investigate your claim.

Downloaded from the University of Groningen/UMCG research database (Pure): <http://www.rug.nl/research/portal>. For technical reasons the number of authors shown on this cover page is limited to 10 maximum.

CHAPTER 5

Modification of supramolecular binding motifs induced by substrate registry

In this chapter, the self-assembly properties of two porphyrin isomers on Cu(111) are studied at different coverages by means of Scanning Tunneling Microscopy. The work presented here was done in collaboration with the group of Prof. François Diederich, at the ETH Zürich.

5.1 Introduction

Organic nanomaterials are expected to be of critical importance for the construction of nanodevices to address tomorrow's challenges in electronics, opto-electronics, photonics, and energy and information storage [Gri05][Zha08][Fuk08][Ari08]. Self-assembled supramolecular layers on surfaces, obtained from highly programmed molecular entities, are anticipated to play a leading role in the development of these future devices. For their fabrication, it is necessary to have a detailed understanding on how self-assembled structures are built up, and even more so, on how their building blocks can be designed in a way to generate predictable architectures and display all features requested for future applications. Furthermore, knowledge on substrate reactivity is essential, since differences in substrate reactivity can lead to very different behavior of adsorbed molecules [Zan90][Tau07]. Scanning tunneling microscopy (STM) has made the direct observation of molecular assemblies on solid surfaces possible, which caused a major break-through towards understanding the complex interactions in an assembly, both between the adsorbed molecules as well as between molecules and substrate [DeF03][DeF00]. Porphyrins proved on many occasion to be the perfect building blocks to construct such molecular devices, as they are inexpensive, easy to modify, and possess a rigid, defined geometry. As a key feature, porphyrins prefer lying flat on metal substrates, due to their extended π - system that is in strong contact with the surface. Continuing our studies on differently modified porphyrins and their behavior on surfaces, we started from an already known Zn^{II} porphyrin, that had been studied extensively on Cu(111) [Win08] and, in the free-base form, on Au(111) [Yok01]; and we

elongated each of the two *meso*-bound, *trans*-oriented 4-cyanophenyl substituents of this molecule by one phenylene unit (Figure 5.1b). Additionally we synthesized the same extended porphyrin with two 4'-cyanobiphenyl groups in an angular *cis*-orientation (Figure 5.1a). Here we report on the various intermolecular interaction motifs in supramolecular assemblies of the *cis*- (**1**) and *trans*- (**2**) bis(4'-cyanobiphenyl) Zn^{II} porphyrins on Cu(111) surfaces.

5.2 Conformation of porphyrins on surfaces

Crystalline *meso*-phenyl-substituted porphyrins usually feature a nearly planar porphyrin macrocycle with the phenyl rings adopting an approximately orthogonal orientation towards this plane. In solution, rotation about the C–C bond connecting the porphyrin and phenyl rings is strongly hindered. Out-of-plane distortions of the *meso*-phenyl have been observed for crystalline 4-cyanophenylporphyrins, with the tilt angle between the porphyrin plane and the straight line passing through C_{1_{ph}} – C_{4_{ph}} – C≡N amounting up to 10° [Bon02]. In crystalline tetrakis(4-cyanophenyl)–Zn^{II}–porphyrin, the 4-cyanophenyl rings are orientated orthogonally to the porphyrin macrocycle and undergo intermolecular, dipolar C≡N⋯H–C_β contacts with pyrrolic hydrogens of neighboring molecules in the crystal lattice [Kri98].

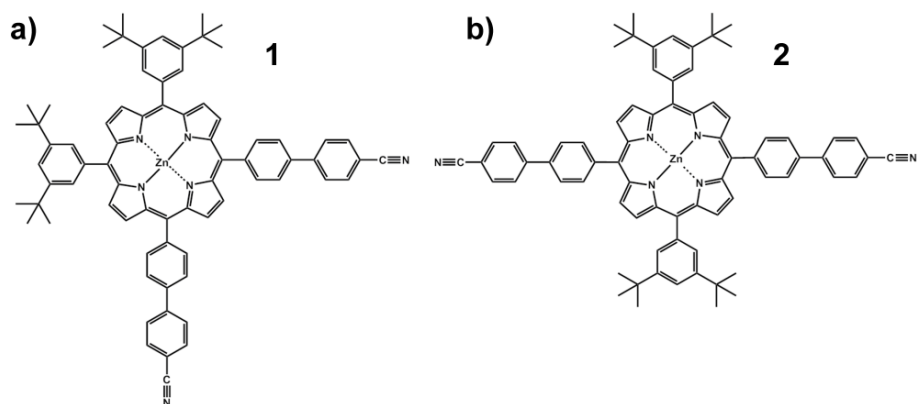


Figure 5.1. Molecular model of (a) *cis*- (**1**) and (b) *trans*- (**2**) Zn^{II} porphyrin isomers.

Whereas *meso*-substituted porphyrins are rather rigid in the bulk and in solution, with conformational preferences as described, if deposited on metal surfaces, strong substrate interactions induce deformations to the overall structures that are not observed in the liquid and crystalline state. Calculations from STM images of tetrakis[3,5-di(*tert*-butyl)-phenyl]- Co^{II} -porphyrins on Ag(111) show a substantial out-of-plane tilt angle of 25° of the *meso*-phenyl rings with respect to the porphyrin plane, compared to the 10° tilt seen in the crystal [Buc07].

Furthermore, the intermolecular interaction motifs change on surfaces. Thus, the two-dimensional assembly of the bis(4-cyanophenyl) analogue of **2**, obtained on Au(111) surface under UHV conditions, was shown by STM to involve antiparallel dipolar $C \equiv N \cdots C \equiv N$ interactions as well as additional, hydrogen-bond-type $C \equiv N - C_{ortho}$ interactions involving the positive polarized hydrogen ortho to the CN group (see Figure 5.3 below) [Yok01]. This bonding motif requires the *meso*-phenyl rings to rotate away from their

preferred perpendicular conformation and strive for closer coplanarity with the porphyrin macrocycle, an effect which is exclusively observed on surfaces due to strong interactions between the porphyrin core and the substrate [Jun97]. The rotation induces steric repulsion between the *meso*-phenyl hydrogens and the β -hydrogens of the porphyrinic core, resulting in a saddle-shaped deformation of the macrocycle [Yok01]. High-resolution UHV-STM, as shown in Figure 5.2 for *cis*-isomer **1**, allows observation of this phenomenon by imaging the porphyrin core as two oblong protrusions where two opposite pyrrole rings are pointing upwards, separated by a dark line representing the two rings that are twisted downwards. Due to the different nature of the porphyrin substituents, their identification by STM is straightforward: bulky 3,5-di(*tert*-butyl)-phenyl side groups are visible as two bright circular spots of two sizes, whereas the rod-like 4'-cyanobiphenyl substituents appear as short lines with distinctively less intensity (Figure 5.2) [Yok04]. Since the upwards-pointing *tert*-butyl group of the 3,5-di(*tert*-butyl)phenyl substituent is forcing the pyrrole ring downwards, this group appears brighter than the other *tert*-butyl group close to the upwards-facing pyrrole ring. On the basis of this assignment of the orientation of the substituents, two conformational isomers of the *cis*-isomer can be identified: “Type **A**” is characterized by the bending line separating the 4'-cyanobiphenyl from the 3,5-di(*tert*-butyl)-phenyl substituents and “type **B**” is characterized by the bending line being on the symmetry axis of the molecule. In *trans*-porphyrin **2** due to its point symmetry, this deformation does not lead to achiral conformational isomers, but instead to conformational enantiomers (i.e., mirror images).

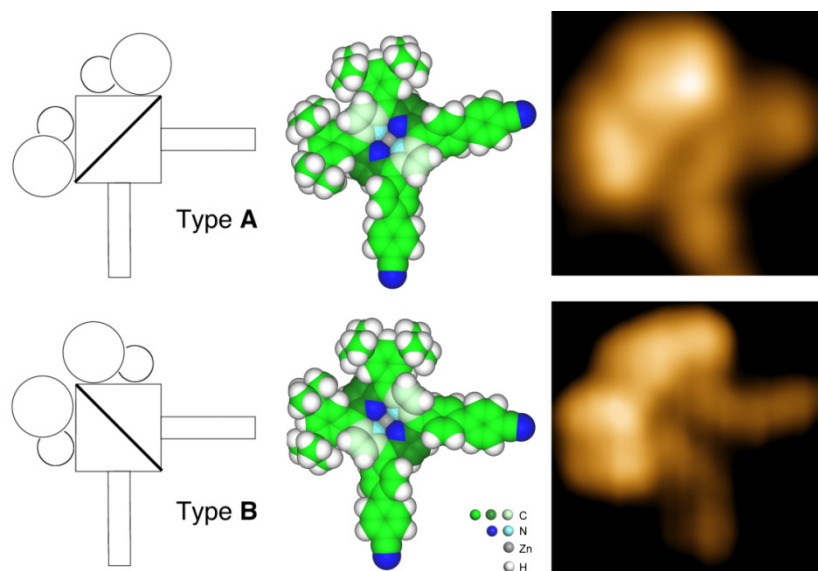


Figure 5.2 Conformational isomers *A* and *B* of *cis*-porphyrin **1** with the “dark line” representing the two corner pyrrole rings that are twisted downwards (light green), whereas the other two corners are twisted upwards (dark green). This phenomenon is induced through the 3,5-di(*tert*-butyl)phenyl substituents twisting sideways; therefore as a second artifact, the *tert*-butyl groups on top of the downwards-bent pyrrole ring appear bigger and brighter, while the other *tert*-butyl group appears smaller.

5.3 The C-H \cdots N binding motif

The hydrogen-bond $C_{sp^2} - H \cdots N \equiv C$ interactions featured by associating cyanophenyl rings are substantially weaker than classic hydrogen bonds involving more acidic O–H, S–H, or N–H H-bond donors. Therefore, they compete with other weak interactions, such as C–H \cdots O, $\pi - \pi$, halogen–halogen, and C–H \cdots π interactions, in solution, in the solid state, and in surface assemblies. Whereas classic hydrogen bonds are highly directional and therefore can organize molecules into networks with predictable architectures

[Pal08] [Bar05] [Des02], the weak $C_{sp^2}-H\cdots N\equiv C$ hydrogen bonds can form in several competing binding alternatives, as displayed in Figure 5.3 [Mal06]. This makes two- and three-dimensional structures built upon $C_{sp^2}-H\cdots N\equiv C$ interactions harder to predict, but offers the advantage that this binding motif is able to adapt to very different geometries. Therefore, numerous types of association patterns are possible, whereas those based on classic hydrogen bonds are geometrically very limited. On metal substrates, geometries a) and b) have been observed for two-dimensional assemblies [Yok01] [Win07], with b) being preferred for porphyrins with *meso*-4-cyanophenyl groups in *trans*-orientation, and a) for porphyrins with *meso*-4-cyanophenyl groups in *cis*-orientation. Furthermore, geometry c) has been observed for chain-like structures where the substrate determined a rotation of 120° between two neighboring (*meso*-cyanophenyl)- Zn^{II} -porphyrins, resulting in intermolecular $C-H\cdots N\equiv C$ interactions (Figure 5.3c, with $\Theta=180^\circ$) [Win07].

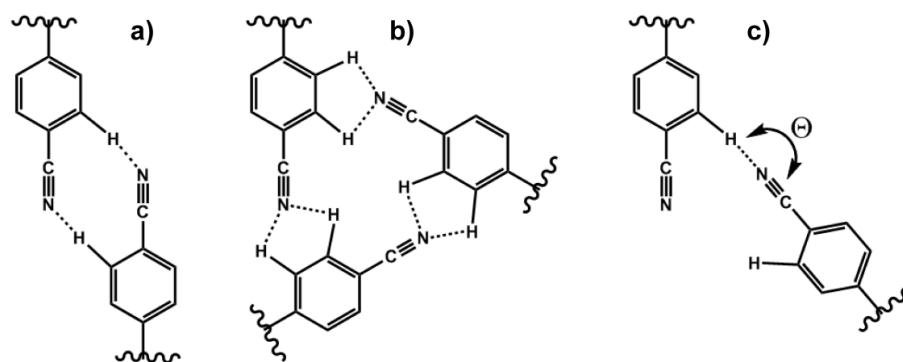


Figure 5.3. Typical $C-H\cdots N$ interactions between cyanophenyl moieties: a) antiparallel dipole-dipole bonding, b) trimeric bonding, and c) hydrogen bonding-type association, where the angle Θ is variable.

5.4. Formation of oligomeric self-assembled macrocycles by *cis*-isomer 1

Upon deposition of the *cis*-isomer **1** onto a Cu(111) surface at sub-monolayer coverage, the porphyrins build up oligomeric structures. Unlike previous work from Yokoyama et al., where a similar molecule with shorter 4-cyanophenyl binding groups was forming exclusively tetramers on a Au(111) substrate [Yok01], here everything from dimeric to hexameric as well as chain-like structures could be observed. We assign this structural diversity mainly to the following effects. Firstly, as introduced before, the antiparallel CN...CN dipole-dipole bonding motif was observed to be the most preferred arrangement of two 4-cyanophenyl groups on a gold substrate (Figure 5.3) [Yok01], but the cyanophenyl groups can also interact in different geometries (Figure 5.3b and c), provided that the accompanying loss in dipolar-bonding energy is compensated by another contribution. Secondly, it has been shown that the interaction strength of large aromatic molecules [that is, 3,4,9,10-perylenetetracarboxylic dianhydride (PTCDA)] with a noble metal substrate decreases in the order Cu(111) > Ag(111) > Au(111) [Tau07]. Thus, a substrate change is expected to influence the delicate balance between adsorbate-adsorbate and adsorbate-substrate interactions in such a way that the adsorption position of the molecule together with its conformational state and intermolecular-bonding pattern will be altered. This corresponds well to our former studies, where simultaneous imaging of similar porphyrins and Cu(111) substrate atoms showed that the porphyrins are oriented

on the surface with their characteristic dark line aligning with one of the three principal directions of the substrate [Win07].

Although macrocyclic oligomers ranging from dimers to hexamers have been observed in our data, there was a clear preference visible for the formation of trimers and tetramers (Figures 4a and 6). We associate this behavior to the above discussed strong adsorbate–substrate interactions, inducing all porphyrins to align with their dark lines along one of the three principal directions of the Cu(111) substrate (Figure 5.4a). Trimers showed to be one of the most “straightforward” forms of assembly in that they are observed to consist almost exclusively of all-type **A** conformational isomers, with only few all-type **B** trimers observed. This preference for same-type trimers is readily explained by the fact that in order to form a triangular cluster, same-type porphyrins arrange in such a way that their dark lines adopt three different orientations separated by rotations of 120° , which nicely corresponds to the three principal directions of the Cu(111) substrate (Figure 5.4c). This accordance with the lattice makes up for the fact, that despite the triangular geometry, the CN substituents do not bend towards an angle of 60° to adopt a perfectly antiparallel bonding motif. Instead, they keep their preferred rectangular shape and display a mixed, about 150° bonding motif, between antiparallel $\text{CN}\cdots\text{CN}$ and $\text{C}\equiv\text{N}\cdots\text{H}-\text{C}$ hydrogen-bonding interactions. Hence, if there is some distortion, it is not substantial enough to be recognized with STM. Yet, for the trimers the clear preference seen for type **A** assemblies might be due to a small difference in energy between type **A** and **B** molecules for the case that the 4'-cyanobiphenyl substituents are indeed slightly bent towards each other, invisible for STM.

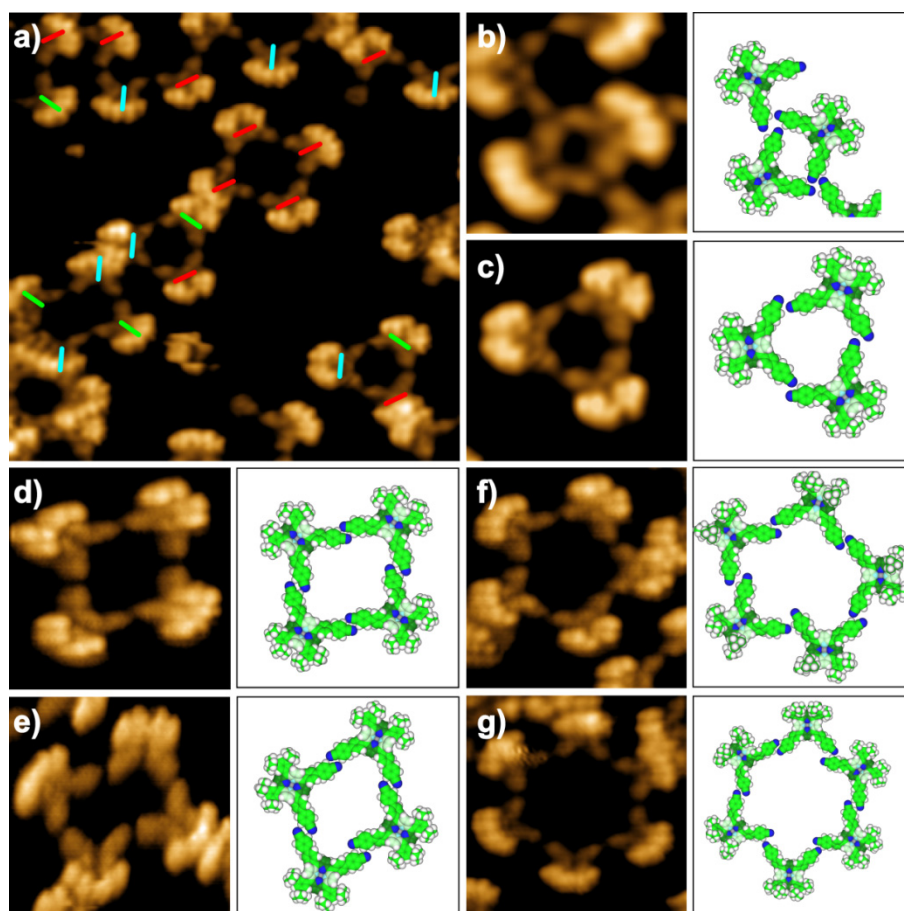


Figure 5.4. STM images for *cis*-porphyrin **1** on Cu(111). a) Detailed image ($18 \times 18 \text{ nm}^2$) showing different oligomeric structures from which the orientation of the porphyrins with respect to the substrate can be identified. b)–g) Detailed STM images with the corresponding molecular models for the different oligomeric structures (image size given in brackets): b) dimer ($5 \times 5 \text{ nm}^2$) c) all-type **A** trimer ($6.3 \times 6.3 \text{ nm}^2$); d) mixed-type tetramer ($6 \times 6 \text{ nm}^2$); e) all-type **B** tetramer ($6.2 \times 6.2 \text{ nm}^2$); f) irregular pentamer ($7.6 \times 7.6 \text{ nm}^2$); g) regular hexamer ($8.2 \times 8.2 \text{ nm}^2$). The surface-induced deformation is denoted by darkening/lightening the respective down-or upwards bent pyrrole groups.

The tetramers observed on the Cu surface can be divided into two subgroups: on the one hand there are the same type tetramers (Figure 5.4e), and on the other hand we see mixed tetramers showing

alternating type **A** and **B** molecules (Figure 5.4d). Furthermore, same-type tetramers look slightly distorted in our STM data, with the 4'-cyanobiphenyl substituents not meeting in the optimal 180° angle, despite the geometric possibility given by the molecular shape. Mixed-type tetramers on the contrary, are shown to build up regular rectangles and interact via antiparallel CN...CN dipole–dipole bonding. This difference in behavior between same-type and mixed-type tetramers is again attributed to the Cu(111) substrate demanding exact alignment of the porphyrin dark lines onto the three Cu(111) main axes. Therefore, mixed-type tetramers (Figure 5.4d) contain porphyrins, in which dark lines are aligned parallel to each other along the same axis. Thereby the 4'-cyanobiphenyl legs are in an unstrained 180° angle, which allows them to undergo optimal antiparallel dipolar bonding. At the same time, porphyrins in a same-type tetramer stick to the surface with their dark lines drawing a substrate-induced angle of 120° and for that reason cannot optimally interact with one another. This effect accounts for the overall distorted structure, with two inwards and two outwards bent dipolar supramolecular synthons (Figure 5.4e). It has to be mentioned further that, contrasting the trimer case, in the tetramer subgroup of same-type assemblies, where the substituents have to bend outwards a little, all-type **B** seems to be much preferred over all-type **A**. Therefore, we contemplate that while porphyrins with legs that are slightly inwards bent prefer type **A**, porphyrins with slightly outwards bent legs prefer type **B**.

Pentamers are very rarely observed, which meets the expectations, since the pentagonal structure neither fits the Cu(111) lattice nor the 90° angle between binding substituents in the porphyrin. Therefore, observed pentamers are not regular; the porphyrins are

interacting with each other in different ways, and type **A** and **B** porphyrins come together randomly in one structure, yet with their dark lines always sitting along one of the three Cu(111) main orientations (Figure 5.4f).

Hexameric structures are favored again by the Cu(111) geometry, nevertheless they already show the limitations in building up rather big regular hollow structures: even if the position of the porphyrins is restricted to one of the three dimensions of the copper lattice, they enjoy some degree of freedom. As a result of the few observed hexamers, one rarely sees one that is a completely regular same-type assembly with all porphyrins undergoing the same $C \equiv N \cdots H - C_{sp^2} - H$ bonding (Figure 5.4g). Once again, only all-type **B** regular assemblies are observed, since the substituents are expected to slightly bend outwards. More often than seeing regular assemblies, it is observed that one molecule of the circle switches type in order to undergo antiparallel $C \equiv N \cdots C \equiv N$ bonding with one neighbor, and $C \equiv N \cdots H - C$ H-bonding with the other. Also observed were hexamers where one molecule folds inwards, presumably for bonding angle optimization, or with an extra molecule occupying the ring cavity to expand two binding sites towards a preferred trimeric pattern.

The dimer represents one of the most interesting structures observed in the course of this study. One would expect dimer formation to occur between two same-type molecules via a bonding pattern observed before in a trimeric arrangement, where the CN group of one porphyrin points towards both aromatic hydrogens of the neighbor's 4'-cyanobiphenyl group. This arrangement would allow the two molecules to keep the substituents in optimal perpendicular conformation towards

each other (Figure 5.4b). However, this is exclusively observed if another substituent is coming from the side to complete the trimeric motif (Figure 5.4b). Upon heating to elevated temperatures $>150\text{ }^{\circ}\text{C}$, instead, the 4'-cyanobiphenyl substituents of porphyrin dimers seem to bend towards each other until they no longer stand perpendicular, but are now drawing an estimated angle of 60° (Figure 5.5d). This means that the two 4'-cyanobiphenyl substituents are each bent about 15° away from their preferred rectangular position towards each other ($(90-60)/2=15^{\circ}$). Such a strong distortion away from the favorite 90° angle between substituents is unprecedented in porphyrin chemistry, and no studies on the lateral flexibility of porphyrin substituents have been performed to date. Presumably, the two substituents can only bend towards each other in such a way, due to two major effects. First of all, as previously pointed out, the saddle-shaped deformation of the porphyrin ring induced by the strong interactions with the copper substrate causes the pyrrole ring between the 4'-cyanobiphenyl residues, which would usually prevent such a rapprochement by steric repulsion, to twist up- or downwards and give way to the two legs to come closer together. Without this surface-induced deformation, lateral movements of the substituents would not be possible. Second, and even more important, this yet unknown lateral distortion of the *meso* substituents of about 15° each can be attributed to the coordination of two cyano groups of opposite molecules towards a single Cu adatom. It is known that at elevated temperatures the Cu step edges become mobile and thus, the Cu adatoms required for dimer formation are available [Lin02]. In all likelihood, the gain in energy with two cyano groups involved in coordination bonding to a Cu adatom makes up for the molecular distortion (Figure 5.5c). While at lower temperatures, no

dimers of this kind could be found due to the insufficient amount of (thermal) energy to enable the lateral movements of the substituents, annealing at 150 °C is sufficient for the formation of Cu-coordinated dimers (Figure 5.5a). Along this line, even more dimers appeared upon heating to 200 °C (Figure 5.5b).

Coexistence of different porphyrin conformers have been already observed for a tetrakis(*meso*-aryl)-substituted porphyrin on a Cu(111) substrate, which adjusts to a crystal lattice mismatch by mixing different unusual conformational isomers [Hill06]. Additionally, the elongation of the binding substituent from 4-cyanophenyl to 4'-cyanobiphenyl offers even more tolerance for distortion, as more bond angles can be bent to adjust to diverse spatial arrangements. Most molecules involved in this kind of dimer formation are type **A**, which again confirms the hypothesis derived from the trimers, same-type tetramers, and hexamers, that **A** is rather preferred when the cyanobiphenyl substituents are bent towards each other, while **B** is favored when the legs are bending apart.

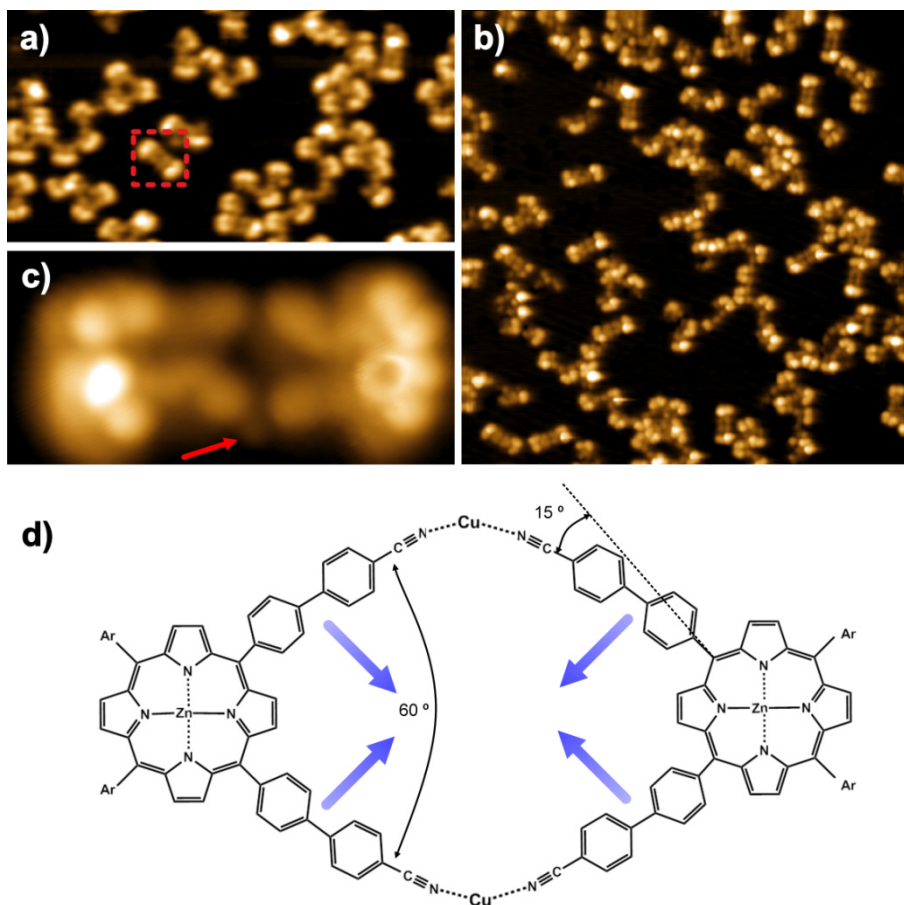


Figure 5.5. a) STM image ($50 \times 26 \text{ nm}^2$) for submonolayer coverage of **1** on Cu(111) annealed at $150 \text{ }^\circ\text{C}$. A few dimeric structures can be observed. The red square marks a dimer that is enlarged in c). b) STM image ($60 \times 60 \text{ nm}^2$) for submonolayer coverage of **1** on Cu(111) after annealing at $200 \text{ }^\circ\text{C}$. Now, mainly dimeric structures can be observed. c) High-resolution STM image ($5.5 \times 2.5 \text{ nm}^2$) of the dimer marked by the red square in a). A copper atom is visible in between two substituent legs (red arrow). d) Simplified model of the two 4'-cyanobiphenyl groups bend together by ca. 15° each in order to undergo coordination bonds to two Cu atoms. Ar = 3,5-di(*tert*-butyl)phenyl.

5.5 Coverage dependence of the most abundant macrocyclic structures formed by *cis*-isomer 1

At a coverage of 0.25 ML (ML=monolayer), mainly trimeric and tetrameric structures are observed. Tetramers are slightly preferred, which might be due to the fact that this geometry is the only one rendering antiparallel dipolar bonding possible without distortion of the substituents. No dimers are present at this coverage; few hexameric structures and barely any pentamers are observed. When increasing the coverage up to 0.5 ML, trimers and tetramers still are the major fractions, though trimers now are slightly more favored than tetramers, presumably because they encircle a smaller area. Hexameric and pentameric structures are becoming more frequent, and the first dimers appear on the surface. At a coverage of 0.75 ML, the preference of trimers over tetramers becomes even more apparent. No hexameric and pentameric structures are observed, while dimers continue to get progressively more popular (Figure 5.6).

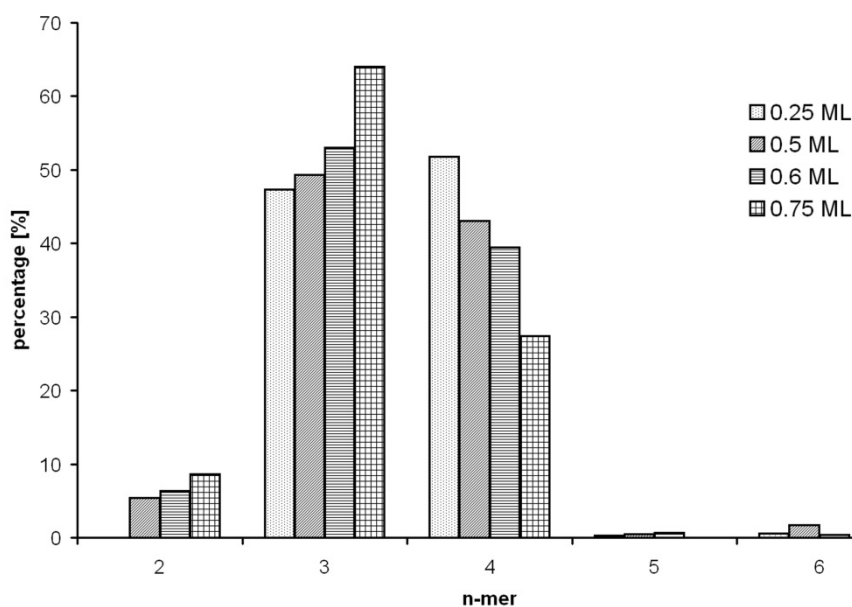


Figure 5.6. Analysis of the frequency for the appearing macrocyclic oligomer structures in dependence of the total molecular coverage, with n being the number of porphyrins involved, plotted against the percentage of occurrences at a given coverage. ML=monolayer.

Upon further increase of the coverage, the available space decreases and structures with smaller encircled space become favored. This effect to opt for the most compact arrangement reaches its maximum at coverage > 0.75 ML. As expected, there was no regular network formation observable; the molecules started to form an irregular assembly incorporating macrocyclic oligomers, irregular curvy chains, and extensive branching.

5.6 A broad spectrum of self-assembled structures of *cis*-isomer **1** influenced by molecule–substrate interactions

While investigating the arrangement of *cis*-bis(4'-cyanobiphenyl)-substituted Zn^{II} porphyrins on Cu(111) and observing the very strong directing force of the substrate, we could not help but notice that this indeed did not occur in the work of Yokoyama and co-workers, who investigated the formation of tetramers for a very similar *cis*-bis(4-cyanophenyl) porphyrin, yet on a Au(111) surface [Yok01]. In contrast to our findings, Yokoyama et al. observed only tetramers (cf. Section on the formation of oligomeric self-assembled macrocycles by *cis*-isomer **1**), and they consisted exclusively of type **A** porphyrins [YokP]. Yet, these same-type tetrameric assemblies displayed regular antiparallel CN⋯CN binding and porphyrin dark lines in a 90° angle towards each other. This alternation of dark lines on Au(111), not fitting the geometry of the gold lattice, occurs solely due to molecular conformational preferences, and the influence of the substrate is negligibly small [Yok01] [Yok04]. This discrepancy is again explained by the increase of adsorbate–substrate interactions; while Yokoyama worked on a less interacting Au(111) surface, where the molecules interact in their one preferred bonding motif, the Cu(111) substrate demands exact alignment of the porphyrin's dark lines onto the Cu(111) main axes. The Cu(111) substrate directs the porphyrin molecules and, due to this strong registry effect, can thus give rise to a much broader array of possible structures, also including weaker intermolecular bonding patterns.

5.7 Assemblies of *trans*-isomer **2** on Cu(111)

Deposition of *trans*-isomer **2** at low coverage leads to the formation of linear chains, which were sometimes interconnected by a trimeric branching pattern (Figure 5.7a+b). The molecules along a chain are connected by antiparallel dipole–dipole interactions of their 4'-cyanobiphenyl substituents. Among identical enantiomers, two molecules of **2** can bind in a linear fashion (where the dark lines are parallel, Figure 5.7c, 1+2, and 3+4) or with a kink (where the dark line of the second molecule is oriented along one of the two other Cu(111) axes, Figure 5.7c, 2+3). This is in correspondence with our earlier studies as well as with the requirement of the two downwards twisted pyrrole rings to sit on one of the three main Cu(111) directions [Win07] [Win08]. The trimeric branching pattern is caused by antiparallel CN...CN interactions together with $C\equiv N\cdots H-C_{sp^2}$ H-bonding interactions, resulting in a cyclic arrangement of the cyano groups (Figure 5.7b) [Yok01]. Both observations corresponded nicely to patterns found for a similar *trans*-bis(4-cyanophenyl)-substituted molecule in our previous studies [Win08].

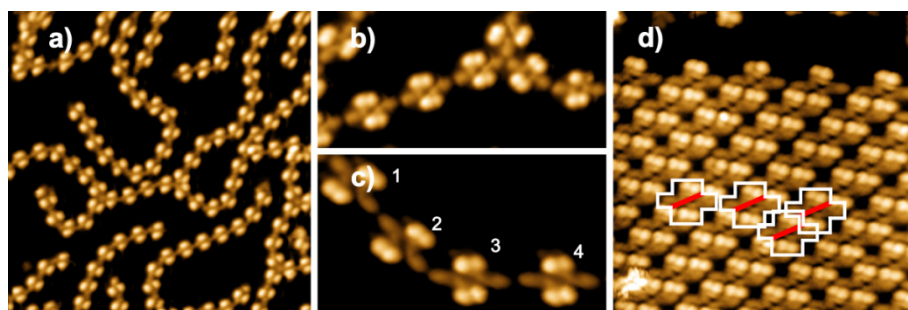


Figure 5.7. STM image ($50 \times 50 \text{ nm}^2$) at low coverage of **2** on Cu(111); b) Cut-out ($15 \times 7 \text{ nm}^2$) showing a trimeric branching site; c) Cut-out ($10.4 \times 5.7 \text{ nm}^2$) showing the bonding between two identical conformational enantiomers with their dark lines along the same direction (1+2, and 3+4), as well as between two identical enantiomers with their dark lines along different directions (2+3); d) STM image ($15 \times 15 \text{ nm}^2$) of *trans* isomer **2** on Cu(111) at high coverage showing the 2D arrangement of a dense, non-porous network (molecules encircled in white, dark lines assigned in red).

On Au(111) at low coverage, porphyrins with only one 4-cyanophenyl substituent were observed to interact exclusively via the trimeric bonding motif, whereas porphyrins with two *trans*-(4-cyanophenyl) substituents, that is, two binding sites, formed solely chains via antiparallel dipole–dipole bonding [Yok01]. Instead, for a *trans*-bis(4-cyanophenyl)–Zn^{II}–porphyrin on Cu(111) both trimeric and antiparallel bonding was observed [Win07]. This shows again, as seen before for *cis*-porphyrins, that depositing similar molecules on Au(111) gives rise to only one, the thermodynamically most preferred, structure, whereas Cu(111) as a substrate supports the molecules and allows them to interact in a variety of ways.

In contrast to our previous work, at high surface coverage, no hexagonal porous network was building up upon deposition of *trans*-isomer **2** onto the Cu(111) surface. Instead, an adlayer was observed,

consisting of interlocked chains (Figure 5.7d). A similar type of network was so far only observed for porphyrins held together by classic hydrogen bonding on Au(111), which induces a linear geometry [Yok04], but not for flexible binding motifs such as the dipolar and weak H-bonding- type interaction between cyanophenyl residues. It is assumed that for a hypothetical hexaporous network based on the trimeric motif shown in Figure 5.3b, upon elongation of the substituent from 4-cyanophenyl to 4'-cyanobiphenyl the pore-to-pore distance would be too big and the network would collapse. In the adlayer, the molecules are once more held together only by antiparallel dipole–dipole interactions along one dimension, displaying linear parallel chains as seen at lower coverage. Yet at higher coverage, these parallel chains become interlocked with each other through van der Waals interactions of the voluminous 3,5-di(*tert*-butyl)-phenyl side groups between adjacent porphyrins of two chains, resulting in a further gain of stability. This assembly type can only be constructed from the elongated bis(4'-cyanobiphenyl)- porphyrin; the chains of the bis(4-cyanophenyl)- porphyrin cannot be interlocked, since the gaps between the 3,5-di(*tert*-butyl)phenyl side groups would be too small. Surprisingly, there is one more vital contribution that has to be added to successfully assemble this network: the strong support from the Cu(111) surface. When depositing the bis(4'-cyanobiphenyl)-porphyrin under the same conditions on Ag(111), a less influencing substrate[Tau07], there was no sign of an adlayer of this type.

The surface influence can be observed further, when comparing this adlayer with the before-mentioned similar one held together by classic hydrogen bonds on Au(111) [Yok04]. In this classic hydrogen-bond network, one can see that the molecules are not directed by the

Au(111) surface, since their dark lines are alternating—solely defined by the supramolecular assembly and ignoring the three-fold surface symmetry of the Au(111) lattice. In contrast, the Cu(111) surface influence on the adlayer held together by non-directive dipole–dipole bonds can be even observed by eye, since here the dark lines of all molecules are aligned along one lattice dimension (Figure 5.7d). During the deposition process of the molecules on the hot surface, reorientation of the molecules has taken place. In the subsequent cooling process the adlayer forms, which leads to the segregation of the two enantiomers. The same observation can be made in the porphyrin chains at lower coverage: the porphyrin’s dark lines in a linear chain are alternating on Au(111) [Yok01], whereas on Cu(111) they are parallel (Figure 5.7c). Therefore, the same network geometry can be reached both by a strongly directional bonding motif (such as classic H-bonding) on a less interacting surface as well as by a geometrically flexible bonding motif (such as antiparallel dipole–dipole interactions) on a strongly interacting substrate.

5.8 Conclusions

We have presented a study on the behavior of two porphyrin isomers at lower and higher coverage on a Cu(111) substrate, each isomer containing two rod-like 4'-cyanobiphenyl and two voluminous 3,5-di(*tert*-butyl)phenyl side groups. Remarkably detailed STM images allowed to fully understand the formation of oligomeric macrocycles of *cis*-isomer **1**—a type of nanoislands—at lower coverage on a Cu(111) surface. It was shown how flexible 4'-cyanobiphenyl substituents can

adapt to very different geometries if supported by strong adsorbate–substrate interactions, due to their elongated structure as well as diverse 4'-cyanobiphenyl bonding motifs. In all detected structures on Cu(111), substrate influence was dominating. Comparisons were drawn between our molecules and studies with a *cis*-bis(4-cyanophenyl) porphyrin on a gold substrate. Whereas the porphyrins on Au(111) only formed regular tetramers via antiparallel CN⋯CN dipolar bonding with the “dark lines” (Figure 5.2) ignoring the directions of the gold substrate, our porphyrins on Cu(111) formed everything from macrocyclic dimers to hexamers using an entire set of different bonding patterns, and with all molecules supported and aligned by the substrate.

Although there is a clear preference evident for structures where *cis*-porphyrin **1** is close to its normal rectangular conformation, it was especially impressive to see how two molecules of **1** could form dimers via coordination bonding with single Cu adatoms released from the surface by heating, despite the presence of a substantial strain resulting from the strong bending of the 4'-cyanobiphenyl groups. This new distortion can be attributed to the substrate-induced deformation of the porphyrin, where the pyrrole ring with its outwards-pointing hydrogen atoms is twisted away from in-between the two substituents, therewith releasing the steric hindrance.

trans-Porphyrin **2** builds up very ordered chains with occasional triangular branching. Two identical enantiomers of *trans*-**2**, with their dark lines oriented parallel to each other, were seen to form linear bonding, while the same enantiomers, with dark lines lying on different axes of the lattice, show kinked bonding. At higher coverage, *trans*-isomer **2**, unlike similar porphyrins, was seen to form a very dense non-

porous network on a Cu(111) surface, which was held together by antiparallel dipole–dipole interactions in one dimension, and van der Waals interactions in the other. The same network geometry was reached in the past employing a strongly directing H-bonding pattern on the weak substrate Au(111) [Yok04]. In our case on Cu(111), we build up the same network with a very flexible binding motif, but on a strongly influencing substrate. This network presumably forms for three reasons: firstly, the molecular chains of elongated *trans*-porphyrin **2** fit snugly into one another, and secondly, a hypothetical hexagonal porous network of **2**, analogous to common networks of shorter *trans*-bis(4-cyanophenyl)- porphyrins [Win07], would be unstable due to its critically big pore-to-pore size. But lastly and most astonishingly, the substrate holds the molecules in place, since this adlayer forms only on Cu(111), not on a slightly less supportive Ag(111) surface. Again, the substrate influence is visible, since all dark lines are aligned along the Cu(111) direction, whereas in the classic hydrogen bond lattice on the weaker interacting substrate Au(111) the dark lines alternate against the geometry of the gold lattice.

This reveals the complexity of supramolecular structure formation induced by the delicate balance of the various possible molecule–molecule and molecule–substrate interactions competing with each other on a metal surface. Due to this complexity, the prediction of self-assembled structures via the bottom-up approach remains an immense challenge. Conclusively, the role of the substrate in the design of such novel self-assembled structures cannot be emphasized enough, since it can make the difference between whether a certain network can be formed or not.

Future work will evaluate the possibility to adjust the oligomeric macrocycles formed by *cis-1* to a uniform size through co-evaporating a fitting template, which the molecules then can encircle. Moreover the role of the substrate in supramolecular chemistry on surfaces will be further investigated, therewith making another step towards a complete insight into the requirements to build up predictable self-assembly architectures.